

MATHEMATICAL MODELING OF FIELD DISTRIBUTION OF SP-57 MAGNET FOR MARUSYA EXPERIMENT

*A. A. Baldin, E. E. Perepelkin, V. L. Smirnov, I. P. Yudin*¹

Joint Institute for Nuclear Research, Dubna

In the framework of the differential formulation of the magnetostatical problem, mathematical modeling of the three-dimensional distribution of magnetic field for the SP-57 magnet of the experimental setup MARUSYA (Laboratory of High Energy Physics, Joint Institute for Nuclear Research) is made. Mathematical formulation of the direct magnetostatical problem is given. Numerical procedures and algorithms for calculation of the field using two scalar potentials are described. The results of modeling and comparison of the calculated distribution of the magnetic field with measured data for the field of the SP-57 magnet with a gap of 0.10 m between the poles are presented. The obtained results are used for processing experimental data and modeling magneto-optical systems.

В рамках дифференциальной постановки магнитостатической задачи проведено математическое моделирование трехмерного распределения магнитного поля спектрометрического магнита СП-57 экспериментальной установки МАРУСЯ (ЛФВЭ ОИЯИ). Приведена математическая постановка прямой магнитостатической задачи. Описываются вычислительные процедуры и алгоритмы расчета поля с помощью двух скалярных потенциалов. Представлены результаты расчета и сравнения расчетного распределения магнитного поля с проведенными измерениями поля магнита СП-57 с межполюсным зазором в 0,10 м. Результаты работы используются при обработке экспериментальных данных, а также полезны для моделирования магнитооптических систем.

PACS: 47.11.Bc, 29.30.A

INTRODUCTION

Magneto-optical spectrometer MARUSYA is a multipurpose device for research on extracted beams of the Nuclotron (accelerating complex of the Laboratory of the High Energy Physics, JINR). The specific feature of the physical program on this accelerator is the investigation of deep subthreshold and cumulative processes with measurement of multiplicity, reaction plane, and polarization of colliding nuclei. The magneto-optical system of the spectrometer consists of two quadrupole lenses K100 and ML17 and two dipole magnets SP-40 and SP-57.

For measurement of particles with momenta 0.3–0.8 GeV/c, focusing behind the magnet SP-57 is performed, SP-57 being used as the analyzing and deflecting magnet. For measurement of a momentum range of 0.6–2 GeV/c, the beam is transported behind SP-40, SP-57 is the deflecting magnet, and SP-40, the analyzing magnet.

¹E-mail: yudin@jinr.ru

In this paper, the problem with respect to two scalar potentials was solved for finding three-dimensional magnetic field distribution. The results of comparison of calculated magnetic field distribution and field measurements [1] for the analyzing magnet SP-57 with a pole gap of 0.10 m are presented (Fig. 1).

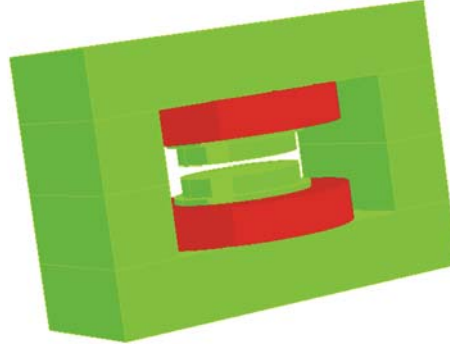


Fig. 1. General view of the spectrometric magnet SP-57

The results are used for processing experimental data; they can also be applied to simulation of other magneto-optical systems.

1. NUMERICAL METHODS

The 3D magnetic field calculation is carried out using the method of two scalar potentials [2]. Solving the boundary value problem (see [2]), we replace derivatives by their difference analogues and assume the magnetic permeability μ constant within one cell and equal to the value at the cell center. We obtain the system of nonlinear equations for determination of the discrete function $u_{i,j,k} = u(i, j, k)$:

$$A_i u_{i+1,j,k} + A_{i-1} u_{i-1,j,k} + B_j u_{i,j+1,k} + B_{j-1} u_{i,j-1,k} + C_k u_{i,j,k+1} + C_{k-1} u_{i,j,k-1} - S_{i,j,k} u_{i,j,k} = 0, \quad (1)$$

where A_i, B_j, C_k, S_{ijk} are the nonlinear functions of $\mu_{i,j,k}$ (i.e., magnetic permeability).

The two-step iterative process was used for solution of this nonlinear system of difference equations (1); in this process, loops of sequential upper relaxation upon potential calculation alternate with lower relaxation for magnetic permeability:

$$\begin{aligned} u_{i,j,k}^{n+1} &= (1 - \omega) u_{i,j,k}^n + \omega u_{i,j,k}^{n+1/2}, \quad 0 \leq \omega \leq 2; \\ \mu_{i,j,k}^{n+1} &= (1 - \eta) \mu_{i,j,k}^n + \eta \mu_{i,j,k}^{n+1/2}, \quad 0 < \eta \leq 1. \end{aligned} \quad (2)$$

Iterations are terminated if the following condition is satisfied:

$$\frac{1}{N_x N_y N_z} \sum_{i,j,k} \left| u_{i,j,k}^{(n)} - u_{i,j,k}^{(n+1)} \right| / \left| u_{i,j,k}^{(n)} \right| < \varepsilon. \quad (3)$$

In the program realizing this algorithm, the value $\varepsilon = 10^{-6}$ is used.

The simulation domain is shown in Fig. 2. The obtained data are represented in the coordinate system in which the axis Z is directed along the beam of primary particles incident on the target, the axis Y , upward perpendicular to the median plane, and the axis X forms the right system. The point of origin of the coordinate system is the center of the magnet SP-57.

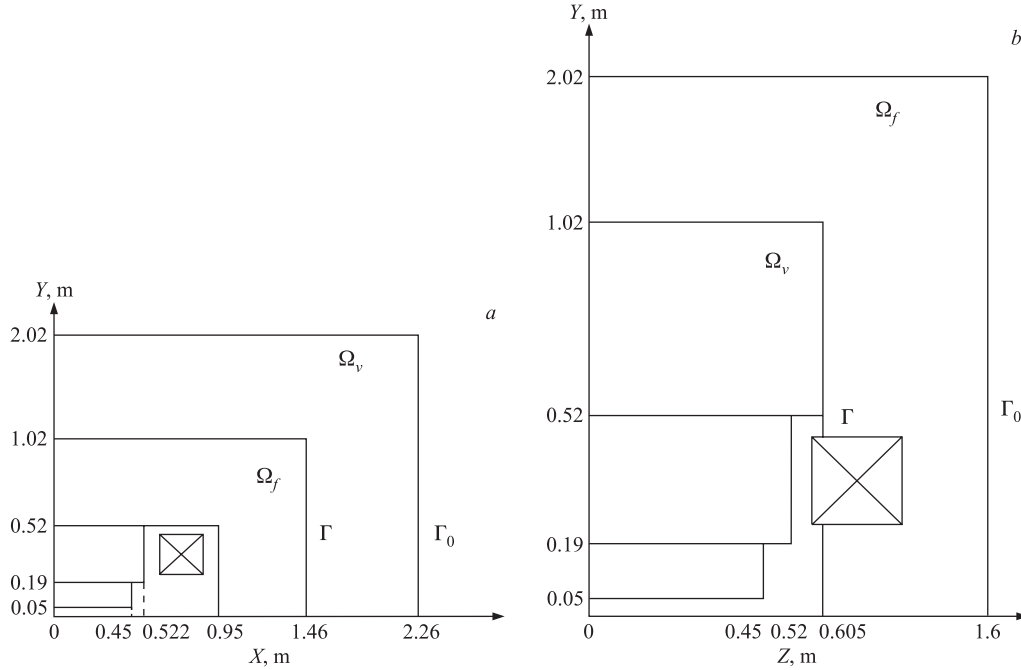


Fig. 2. Numerical domain of 1/8 part of the magnet: a) cut in the plane XOY ; b) cut in the plane YOZ

The numerical grid in the aperture was as follows: for x from 0 to 0.90 m with the step $h_x = 0.01$ m; for y from 0 to 0.10 m, with the step $h_y = 0.01$ m; and for z from 0 to 1.5 m, with the step $h_z = 0.01$ m.

The measurement grid was as follows: for x from -0.64 to 0.56 m, with the step $h_x = 0.02$ m; for y from -0.03 to $+0.03$ m, with the step $h_y = 0.03$ m; and for z from -0.77 to 0.77 m, with the step $h_z = 0.01$ m.

2. NUMERICAL RESULTS

Figure 3 shows the dependences $B_y(x, 0, z)$, $B_y(x, 0.03 \text{ m}, z)$, $B_x(x, 0.03 \text{ m}, z)$, $B_z(x, 0.03 \text{ m}, z)$ for a current of 600 A. In Fig. 3, a, the distribution of the basic field component $B_y(x, 0, z)$ in the median plane is presented. The region of the homogeneous field on a level of 1.743 T is entirely under the magnet pole, the field dropping at the pole edges to 0 G along the beam ($z = 1.50 \text{ m}, x = y = 0$) and in the transverse direction ($x = 0.9 \text{ m}$,

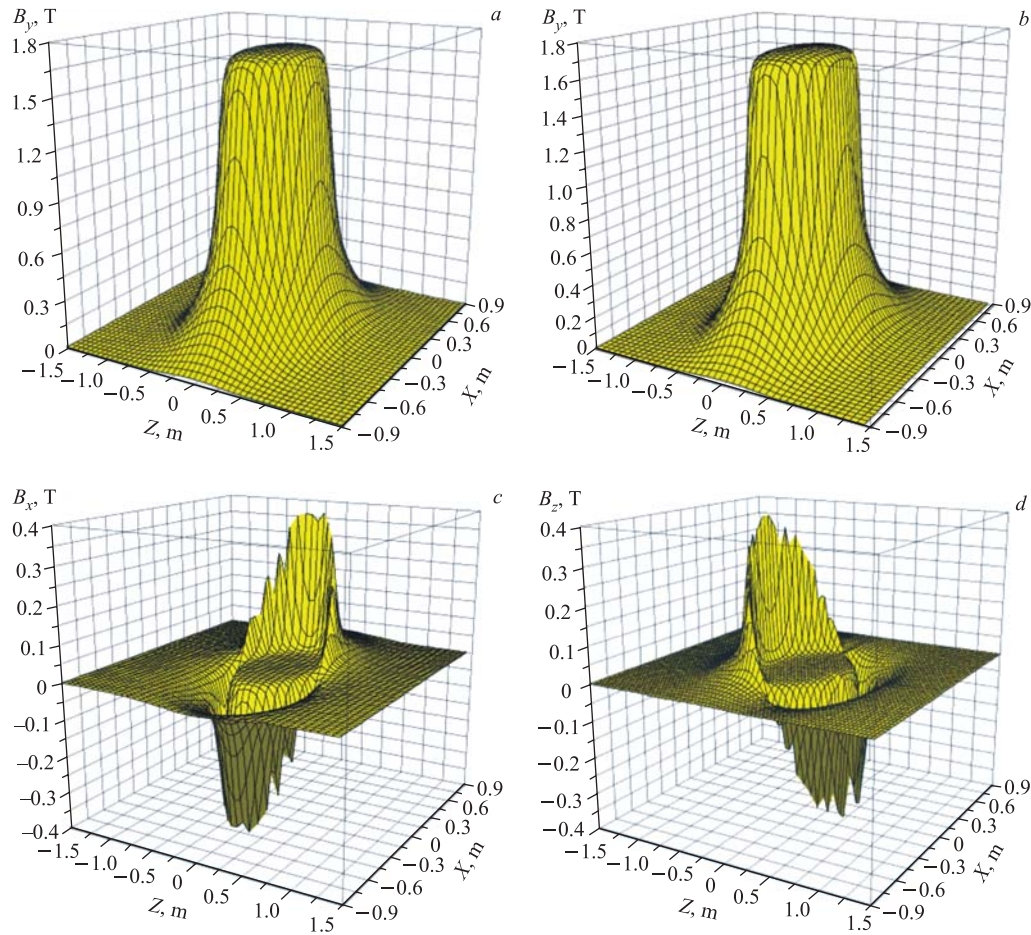


Fig. 3. Spatial distribution of magnetic field components B_y, B_x, B_z for SP-57 and the current $I = 600$ A

$y = z = 0$). In the median plane the other components are equal to zero. In Fig. 3, *b*, the distribution of the basic field component $B_y(x, 0.03 \text{ m}, z)$ in the plane $y = 0.03 \text{ m}$ is shown. The region of the homogeneous field on a level of 1.746 T is also under the magnet pole. Then the field also drops down at the pole edges (both in the transverse direction and along the beam) to 0 G. In Fig. 3, *c*, the distribution of the transverse field component $B_x(x, 0.03 \text{ m}, z)$ in the plane $y = 0.03 \text{ m}$ is presented. In Fig. 3, *d*, the distribution of the longitudinal field component $B_z(x, 0.03 \text{ m}, z)$ in the plane $y = 0.03 \text{ m}$ is shown. The values of magnetic induction components B_x and B_z reach 0.4 T at the magnet edge.

In Fig. 4, the calculated excitation curve $B = B(I)$ for SP-57 is shown for the point with the coordinates $x = y = z = 0$ and a current I from 0 to 600 A.

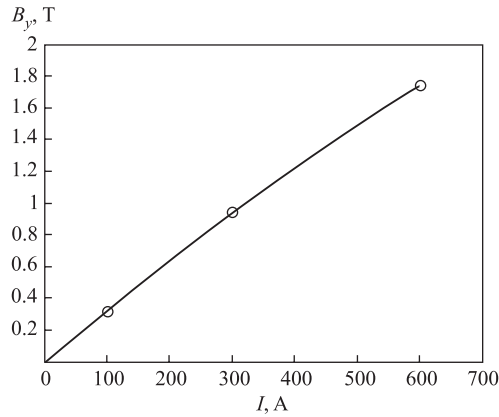


Fig. 4. Excitation curve $B = B(I)$ for the magnet SP-57

3. COMPARISON WITH MEASURED DATA

The plots of comparison of B_y , B_x , B_z for the planes $y = 0$, $y = 0.03$ m depending on Z and X are shown in Figs. 5–8 for the current $I = 600$ A. Hereinafter (see Figs. 5–8), solid lines show experimental quantities; and dashed lines, calculated quantities.

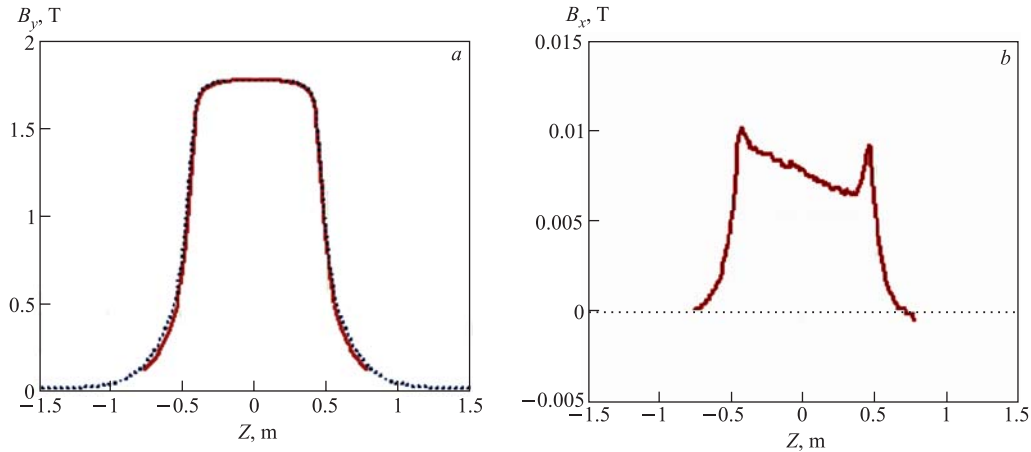


Fig. 5. Distribution of components B_y , B_x for $x = 0$ m, $y = 0$ m (median plane, magnet center)

In Figs. 5 and 6, the distributions of calculated and experimental components B_y , B_x are presented for $x = 0$ m, $y = 0$ m (median plane, magnet center) and the difference of the calculated and experimental main component ΔB_y along the axis Z (along the beam) and along the axis X (in the transverse direction), respectively. The differences ΔB_x and ΔB_z at $y = 0$ are equal to the measured quantities, because the calculated quantities are equal to zero.

In Figs. 7 and 8, the distributions of calculated and experimental components B_y , B_x , B_z are shown for $x = 0$, $y = 0.03$, and the difference ΔB_y along the axis Z (along the beam)

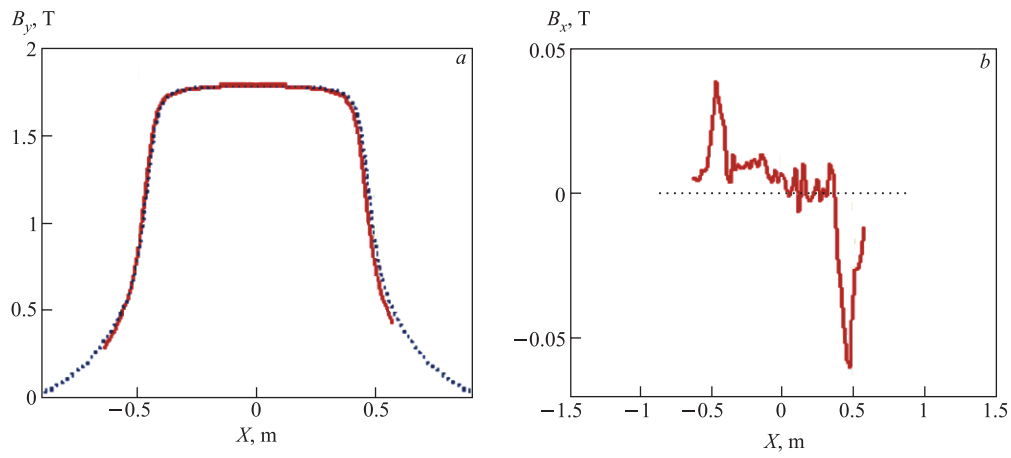


Fig. 6. Distribution of components B_y , B_x for $y = 0$ m, $z = 0$ m (median plane, magnet center)

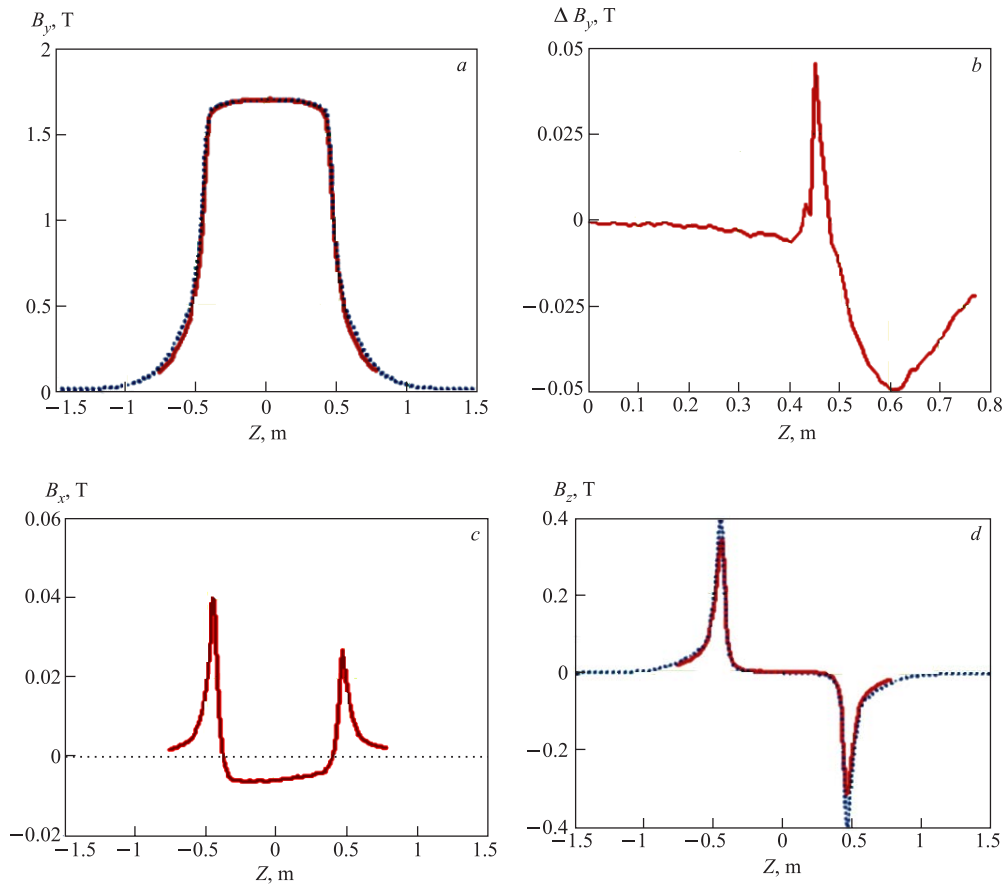


Fig. 7. Distribution of calculated and experimental components B_y , B_x , B_z for $x = 0$, $y = 0.03$ m, and the difference ΔB_y

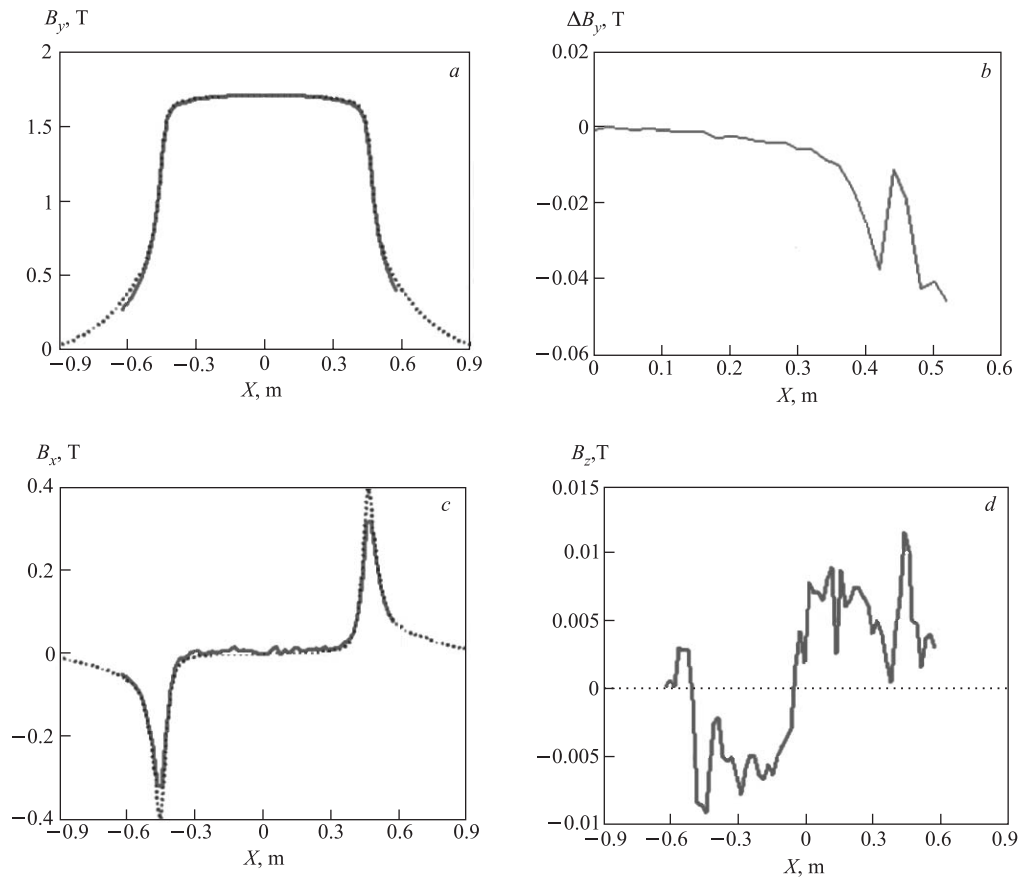


Fig. 8. Distribution of components B_y , B_x , B_z for $y = 0.03$ m, $z = 0$ m, and the difference ΔB_y

and along the axis X (in the transverse direction), respectively. The differences ΔB_x and ΔB_z at $y = 0.03$ m are approximately equal to ΔB_x and ΔB_z at $y = 0$.

CONCLUSIONS

The three-dimensional distribution of magnetic field components for the magnet SP-57 of the MARUSYA spectrometer was obtained numerically for the total aperture.

The results of comparison of calculated and measured [1] magnetic field distribution for the magnet SP-57 were presented. The comparison performed in this paper showed that the error $\Delta B/B \leq 0.5\%$ (≤ 50 G at a level of 1.74 T at the magnet center).

The obtained results are used for computer simulation of the setup and experiment, and in processing physical data.

REFERENCES

1. *Baldin A. A. et al.* Measurement of Magnetic Field Map for Magneto-Optical Spectrometer MARUSYA. JINR Preprint P13-2006-67. Dubna, 2006. 19 p.
2. *Baldin A. A. et al.* Numerical Simulation of the Field Distribution Produced by the SP-40 Magnet of the MARUSYA Setup and Comparison of Simulation Results with Experimental Data // *Zh. Tekhn. Fiz.* 2007. V. 52, No. 11. P. 1397–1406.

Received on April 17, 2009.